permafrost
cci

CCI+ PHASE 2 – NEW ECVS
PERMAFROST

CCN4 OPTION 7
ICEINSAR: INFERRED ACTIVE LAYER WATER/ICE CONTENT AND FREEZE-THAW PROGRESSION FROM ASSIMILATING INSAR IN PERMAFROST MODEL

D2.3 END-TO-END ECV UNCERTAINTY BUDGET (E3UB)

VERSION 1.0

30 SEPTEMBER 2023

PREPARED BY

b·geos GAMMA REMOTE SENSING

NORCE UiO : University of Oslo

Document Status Sheet

Issue	Date	Details	Authors
0.1	18.07.2023	First template	LR
0.2	25.08.2023	First draft to co-authors	LR
0.3	24.09.2023	Second draft to co-authors	LR, LW
0.4	27.09.2023	Review from co-authors and correction	LR, LW, SW
1.0	30.09.2023	Review from all co-authors and correction to final version	LR, LW, SW, AB, TS

Author team

Line Rouyet and Lotte Wendt, NORCE

Sebastian Westermann, UiO

Annett Bartsch, B.GEOS

Tazio Strozzi, GAMMA

ESA Technical Officer

Frank Martin Seifert

EUROPEAN SPACE AGENCY CONTRACT REPORT

The work described in this report was done under ESA contract.
Responsibility for the contents resides in the authors or organizations that prepared it.

TABLE OF CONTENTS

EXECUTIVE SUMMARY

Within the European Space Agency (ESA), the Climate Change Initiative (CCI) is a global monitoring program which aims to provide long-term satellite-based products to serve the climate modelling and climate user community. The two main products associated to the ECV Permafrost are Ground Temperature (GT) and Active Layer Thickness (ALT). GT and ALT are documented by the Permafrost_cci project based on thermal remote sensing and physical modelling.

The Permafrost_cci model takes advantage of additional datasets, such as snow cover and land cover, to estimate the heat transfer between the surface and the underground. However, several challenges remain due to spatially variable subsurface conditions, especially in relation to unknown amounts of water/ice in the active layer that modify the effective heat capacity and the thermal conductivity of the ground. In complex terrain with large spatial heterogeneities, coarse and partly inadequate land cover categorisation, the current results show discrepancies with in-situ measurements, which highlight the need to assimilate new data sources as model input. Although the ground stratigraphy is not directly observable from space, it impacts the dynamics of the ground surface. The seasonal thawing and refreezing induce cyclic subsidence and heave of the ground surface due to ice formation and melt in the active layer, and can therefore be used as indirect indicator of the ground conditions.

Synthetic Aperture Radar Interferometry (InSAR) based on Sentinel-1 images can be used to measure the amplitude and seasonal progression of these displacements. The movement amplitude is related to the amount of water/ice that is affected by a phase change, whilst the timing of the displacement patterns reflects the vertical progression of the thawing/freezing front. Considering the fine to medium spatial resolution of Sentinel-1 images, InSAR time series therefore have the potential to enhance the characterisation of subsurface hydrogeologic and thermal parameters and adapt the existing Permafrost_cci models to improve their performance at the local to regional scale. The *IceInSAR* pilot project (Option 7) will develop a prototype for permafrost model adjustment by assimilating Sentinel-1 InSAR surface displacement maps and time series into the model to constrain stratigraphy parameters. *IceInSAR* will provide pilot products, expected to be used for adjustment of the ECV processing chain of the baseline project in a next phase.

This End-to-End ECV Uncertainty Budget (U3UB) documents the sources of errors and uncertainties of the *IceInSAR* Option 7 products. Methodologies to determine uncertainties of the ground temperature at a certain depth (GTD) and active layer thickness (ALT) products are aligned with the baseline project. The error sources for InSAR are described in detail. It should be noted that error quantification for InSAR SD products is not well constrained especially in permafrost regions where in-situ surface displacement measurements are often lacking. We are exploring methodologies to estimate uncertainties using the interferometric coherence quality measure and indirect methods comparing InSAR results with in-situ data documenting the ground conditions. The methodology for InSAR uncertainty documentation may evolve throughout the project.

1 INTRODUCTION

1.1 Purpose of the document

This document provides an overview of the main sources of uncertainty of the products developed in the Permafrost_cci *IceInSAR* Option 7. It has to be read as a complement to the E3UB from the baseline project [RD-7].

1.2 Structure of the document

Section 2 documents the sources of errors and uncertainties affecting the Option 7 products. Section 3 describes the methodologies to estimate uncertainties. Section 4 summarizes which accuracy will be reported in the final products.

A bibliography complementing the applicable and reference documents (Sections 1.3 and 1.4) is provided in Section 5.1. A list of acronyms is provided in Section 5.2. A glossary of the commonly accepted permafrost terminology can be found in [RD-12].

1.3 Applicable Documents

[AD-1] ESA. 2022. Climate Change Initiative Extension (CCI+) Phase 2 – New Essential Climate Variables – Statement of Work. ESA-EOP-SC-AMT-2021-27.

[AD-2] GCOS. 2022. The 2022 GCOS Implementation Plan. GCOS – 244 / GOOS – 272. Global Observing Climate System (GCOS). World Meteorological Organization (WMO).

[AD-3] GCOS. 2022. The 2022 GCOS ECVs Requirements. GCOS – 245. Global Climate Observing System (GCOS). World Meteorological Organization (WMO).

1.4 Reference Documents

[RD-1] Rouyet, L., Wendt, L., Westermann, S., Bartsch, A., Strozzi, T. 2023. ESA CCI+ Permafrost Phase 2. CCN4 Option 7. IceInSAR: Inferred Active Layer Water/Ice Content and Freeze-Thaw Progression From Assimilating InSAR in Permafrost Model. D.1.1 User Requirement Document (URD). Version 1.0. European Space Agency.

[RD-2] Rouyet, L., Wendt, L., Westermann, S., Bartsch, A., Strozzi, T. 2023. ESA CCI+ Permafrost Phase 2. CCN4 Option 7. IceInSAR: Inferred Active Layer Water/Ice Content and Freeze-Thaw Progression From Assimilating InSAR in Permafrost Model. D.1.2 Product Specification Document (PSD). Version 1.0. European Space Agency.

[RD-3] Bartsch, A., Matthes, H., Westermann, S., Heim, B., Pellet, C., Onaca, A., Strozzi, T., Kroisleitner, C., Strozzi, T. 2023. ESA CCI+ Permafrost Phase 2. D1.1 User Requirement Document (URD). Version 3.0. European Space Agency.

[RD-4] Bartsch, A., Westermann, S., Strozzi, T., Wiesmann, A., Kroisleitner, C., Wieczorek, M., Heim, B. 2023. ESA CCI+ Permafrost Phase 2. D1.2 Product Specification Document (PSD). Version 3.0. European Space Agency.

[RD-5] Bartsch, A., Westermann, S., Strozzi, T. 2023. ESA CCI+ Permafrost. D.2.1 Product Validation and Algorithm Selection Report (PVASR). Version 4.0. European Space Agency.

[RD-6] Westermann, S., Bartsch, A., Strozzi, T. 2023. ESA CCI+ Permafrost. D.2.2 Algorithm Theoretical Basis Document (ATBD). Version 4.0. European Space Agency.

[RD-7] Westermann, S., Bartsch, A., Heim, B., Strozzi, T. 2023. ESA CCI+ Permafrost. D.2.3 End-To-End ECV Uncertainty Budget (E3UB). Version 4.0. European Space Agency.

[RD-8] Westermann, S., Bartsch, A., Heim, B., Strozzi, T. 2023. ESA CCI+ Permafrost. D.2.4 Algorithm Development Plan (ADP). Version 4.0. European Space Agency.

[RD-9] Heim, B., Wieczorek, M., Pellet, C., Delaloye, R., Barboux, C., Westermann, S., Bartsch, A., Strozzi, T. 2023. ESA CCI+ Permafrost. D.2.5 Product Validation Plan (PVP). Version 4.0. European Space Agency.

[RD-10] Bartsch, A., Westermann, S., Strozzi, T. 2023. ESA CCI+ Permafrost. D.2.1 Product Validation and Algorithm Report (PVASR). Version 4.0. European Space Agency.

[RD-11] Heim, B., Lisovski, S., Wieczorek, M., Pellet, C., Delaloye, R., Bartsch, A., Jakober, D., Pointer, G., Strozzi, T. 2021. ESA CCI+ Permafrost. D.4.1 Product validation and intercomparison report (PVIR). Version 3.0.

[RD-12] van Everdingen, Robert, Ed. 1998 revised May 2005. Multi-language glossary of permafrost and related ground-ice terms. Boulder, CO: National Snow and Ice Data Center/World Data Center for Glaciology. (http://nsidc.org/fgdc/glossary/; accessed 23.09.2009).

1.5 Bibliography

A complete bibliographic list that supports arguments or statements made within the current document is provided in Section 5.1.

1.6 Acronyms

A list of acronyms is provided in Section 5.2.

2 SOURCES OF ERRORS AND UNCERTAINTIES

2.1 Error sources in InSAR processing

Various error sources and uncertainties must be considered when using InSAR for measuring surface displacements (SD). They are well documented in reference InSAR literature (e.g. Massonnet and Feigl, 1998; Bamler and Hartl, 1998; Rosen et al., 2000; Rocca et al., 2000; Hanssen, 2001; Kampes, 2006; Ferretti, 2014).

Illustrations of typical InSAR limitations both spatially and temporally are shown in **Figure 1**. With the specific objective to generate the Option 7 SD products, the following elements are especially important to consider:

- **Spatial resolution and averaging of fine-scale processes within InSAR pixels:** The final products are point-based but correspond to the centre point of a *pixel with a specific footprint*. The spatial resolution of SAR images varies according to the sensor (and its acquisition mode). The initial SAR images have a different resolution in azimuth and range direction. The initial ground resolution of the main inputs of the project (Sentinel-1 Interferometric Wide Swath mode) is approx. 5m (range) x 20m (azimuth). Using an 8x2 *multi-looking* factor (averaging looks to provide a better signal quality) we will get a 40x40m resolution. Other higher factors (12x3, 16x4, 20x4) may be tested providing lower resolutions. If the ground conditions are largely heterogeneous within the resolution cell/pixel, InSAR may smooth the results in an unrealistic way and small areas affected by large displacements can be missed by averaging.
- **Vertical projection of one-dimensional measurements:** The analysis of phase changes between two acquisitions at two different times provides information about surface displacements along the *line-of-sight (LOS)* of the SAR sensor. InSAR is only sensitive to displacements that have a component in the LOS direction, which depends on the flying orientation of the satellite (track) and the incidence angle of the radar beam. When focusing on flat terrain, we assume that most of the displacements occur vertically (subsidence during the snow-free season and heave during freeze-back) and the results are therefore projected in this orientation. A slope threshold of 5 degrees is applied based on 20m digital elevation model (DEM) (NPI, 2014). An uncertainty is therefore likely due to possible creeping processes on low-inclined terrain (e.g. solifluction), especially if small topographic variations are missed by the quality/resolution of the DEM. In such cases, the InSAR signal may include a horizontal component wrongly interpreted as subsidence/heave, which may explain local discrepancies between ascending and descending InSAR products.
- **Spatio-temporal relativity of the measurements:** InSAR is a *relative geodetic measurement method*. The InSAR velocity measurements are relative to a chosen area (reference or calibration point). Usually, the operator chooses a point assumed to be stable. However, if this assumption is wrong, the results may be shifted. This is especially a problem if the movement at the reference point is nonlinear (variable in time) as it may differently affect each interferogram (and thus the time series). Due to the lack of available in-situ geodetic measurements in the study areas, we combine three methods to choose a reference point: 1) selection of very high coherence (> 0.8) pixels corresponding to a high signal stability, 2) analysis of orthophotos and geomorphological analysis to identify a bedrock outcrop or a stable man-made structure, 3) iterative approach by testing several reference points and comparing the results to identify displacement shifts.

- **Atmospheric Phase Screen:** A SAR sensor measures the phase difference with accuracy on the order of a fraction of the wavelength; more than accurate enough to be influenced by atmospheric path delay. The so-called *Atmospheric Phase Screen* (APS) is one of the main error sources in repeat-pass InSAR and is mostly due to 1) *turbulent mixing processes* in the troposphere, 2) *stratified tropospheric atmosphere* related to the local topography, 3) differential interaction with *free electrons in the ionosphere* (Hanssen, 2001). Turbulent mixing comes from mixing processes in the inhomogeneous atmosphere, while stratification results from variations in the vertical refractive index profile. The second is correlated with the local topography. Both can be mitigated during the processing using a DEM and spatial-temporal filtering techniques, but unwanted phase components can remain. The Small Baseline Subset (SBAS) algorithm used in the Option 7 mitigates these effects by assuming that atmospheric turbulences are usually correlated in space but uncorrelated in time. By using a redundancy of time-overlapping interferograms, the atmospheric effects can be filtered. However, in seasonal SD products for detecting thaw subsidence and frost heave in Svalbard, few interferograms with short temporal baselines are used at the beginning (May–June) and the end (October–November) of the observation time window due to fast movement and decorrelation. At these periods the results are expected to be noisier than in the middle of the snow-free season (July-September). Errors associated with uncorrected atmospheric effects tend to increase with distance in respect to the reference point and thus affect large areas significantly more than local studies (Emardson et al., 2003).
- **InSAR decorrelation and phase bias:** The phase accuracy in SAR interferometry is affected by decorrelation and noise. Phase decorrelation is due to changes in position of individual scatterers within the resolution cell and is one of the main limitations for successful use of InSAR. Decorrelation is mainly due to either SAR imaging geometric effects (*spatial decorrelation*), or temporal surficial changes (*temporal decorrelation*) (Zebker & Villasenor, 1992). Spatial decorrelation is related to the spatial baseline between the sensor at the different acquisitions. Temporal decorrelation is due to changes in geometrical or electrical properties of the surface, as a function of time between the acquisitions. The interferometric SAR signal will decorrelate when the variability within a pixel is higher than half the wavelength (2.8 cm for Sentinel-1) during the selected time interval. This variability may be caused e.g. by moving parts of vegetation or changes of the land surface. Terrain containing variable liquid water, such as e.g. areas covered with wet snow, will also have different scattering properties from one observation to the next. The scenes affected by (wet) snow are mostly unusable, which reduces the observation time window in cold-climate regions. The temporal decorrelation phenomenon is dependent on the radar wavelength; longer wavelengths are less sensitive to small scale surface scattering changes, but also have a reduced sensitivity to displacement. In addition, despite the use of coherence thresholds to filter out areas affected by decorrelation, the effect of scattering mechanisms in coherent areas must be considered, as the differential propagation of the electromagnetic wave due to changing dielectric properties of the ground may lead to biased phase estimates. This can occur due to snow (Antonova et al., 2016), ground moisture (Zwieback et al., 2015) or vegetation (Zwieback & Hajnsek, 2014). With distributed scattering methods, this issue can be exacerbated when applying low multi-looking factors that tend to overestimate the coherence and thus lead to a filtering that fails to remove unreliable pixels (Bamler & Hartl, 1998).

- **Unwrapping errors and phase aliasing:** An initial interferogram is wrapped, highlighting a succession of fringes when the phase exceeds half the wavelength. The process of restoring the correct multiple of 2π to each point of the interferometric phase image, i.e. to convert the cyclic phase difference into a continuous phase difference, is called *phase unwrapping* and can be performed automatically (Chen & Zebker, 2002). The procedure uses the assumption that the true displacement field has a spatial continuity and thus the spatial variation of the phase is rather smooth. However, if the movement is spatially discontinuous, for example in the case of a localized quick event, unwrapping algorithms can fail to retrieve correct solutions. Areas can be decorrelated due to changes in scattering properties within the resolution cell between the two acquisitions. Such decorrelation effects can contaminate large areas in the interferograms and create discontinuous coherent patches. This makes the retrieval of the absolute phase a challenging task. The interferometric SAR signal can become ambiguous when the displacement gradient between adjacent pixels is higher than a quarter of the wavelength during the selected time interval (phase aliasing). To eliminate time series likely to be affected by this problem, time series with displacements exceeding a quarter of the wavelength (1.4 cm for Sentinel-1) between successive acquisitions were filtered out.

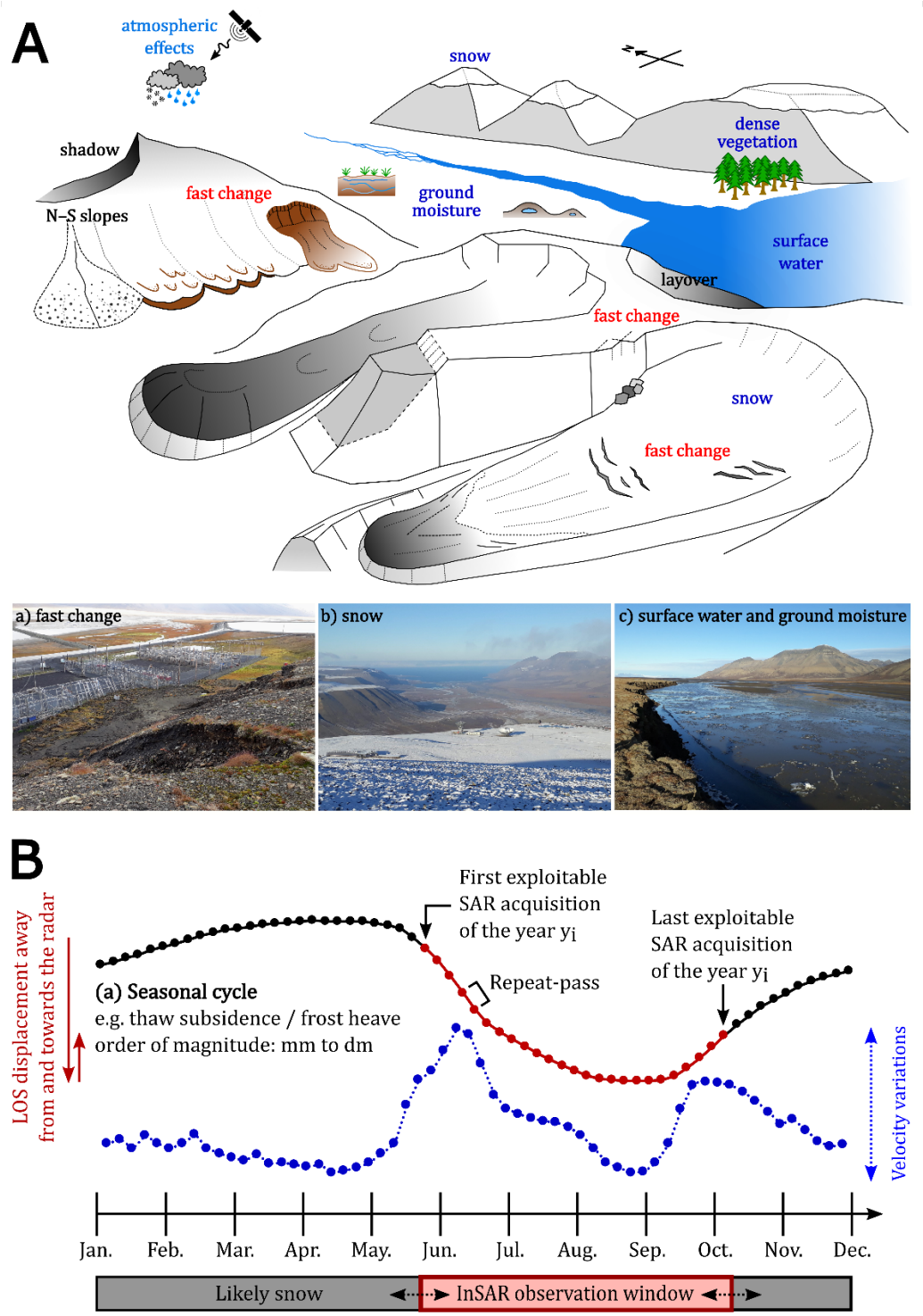

Figure 1. Illustrations of common InSAR limitations in permafrost environments. **A.** Main limitations reducing the InSAR coverage or the reliability of the measurements. Field pictures from central Spitsbergen, Svalbard: **a)** 2017 active layer detachment slide in Longyearbyen; **b)** snow-covered Breinosa mountain top and view over the snow-free valley bottom in September 2019; **c)** flooded Adventdalen bottom in September 2019. **B.** Typical observation window for an InSAR subsidence/heave time series in permafrost lowlands (red line), in respect to the period affected by snow (black line). The expected velocity variation (blue line) determines the applicable temporal baselines to be used to avoid phase ambiguities and temporal decorrelation (modified from Rouyet, 2021).

2.3 Error sources in CryoGrid modelling

The error sources in CryoGrid modelling (both for the Baseline and the Option 7) are related to the quality of the input data and the effect of the algorithm itself (processes that are unaccounted for in the model), as discussed in Langer et al. (2013) for a similar ground thermal model. For ground temperatures, the main source of uncertainty is the insulating effect of the seasonal snow cover, while the thermal properties of the subsurface, especially the uppermost meter, are the most critical parameters for the active layer thickness. An additional source of uncertainty is the driving data sets which we derive by downscaling ERA-5 reanalysis data. The choice of the model algorithm itself also has a certain impact on the results, as demonstrated in Westermann et al. (2023). In the CryoGrid community model, it is possible to select different subsurface model types, so that the magnitude of this model uncertainty can be estimated.

To characterize the uncertainty of such complex multi-parameter models, ensemble methods should be used. At the same time, ensemble methods are the very basis of the data assimilation procedures that will be used in the Option 7. In essence, the data assimilation procedure will not only deliver the "best-guess" model results given the InSAR retrievals for a site, but they will also deliver an uncertainty estimate (see below).

2.3 Uncertainty of validation data

The uncertainty estimates of the validation data are detailed in the baseline E3UB [RD-7]. As a reminder, we here list the main elements to take into account:

- *Ground temperature* accuracy – estimated impact on ground temperature: 0.1K.
- *Sensor depth* accuracy – estimated impact on measurement depth: +/- 2 cm
- *Location* accuracy – estimated impact on location: +/- 200 m
- *Thaw depth* accuracy – estimated impact on thaw depth: 0.02 m
- *Active layer thickness* accuracy – estimated impact on active layer thickness: 0.05 m
- *Location* accuracy of CALM measurement grids – estimated impact on location of the grid centre and or corners: +/- 5 m

3 METHODOLOGY TO DETERMINE UNCERTAINTIES

3.1 Uncertainty of InSAR products

Due to the various error sources affecting the InSAR results (see Section 2.1), the error quantification is a challenging task that is not well constrained especially in permafrost regions where in-situ surface displacement measurements are often lacking. We are exploring methodologies to estimate uncertainties using the interferometric coherence quality measure and indirect methods comparing InSAR results with field data documenting the subsurface properties. The methodology for uncertainty documentation may evolve throughout the project.

In general, the standard deviation of the retrieved velocity depends on the number of interferograms (typically 60–80 per season) and the maximal temporal baseline (48 days) used for the processing. Using the equation 11 from Emardson et al. (2003) and assuming a standard deviation of 5 mm per interferogram due to the atmosphere, the detection capability when using a simple averaging method (stacking) can be estimated to 1.4–1.6 mm/summer. Using SBAS inversion strategies exploiting the redundancy of time-overlapping interferograms to filter out unwanted phase component, the standard deviation is expected to be lower.

The temporal variability of the standard deviation (due to a variable amount of interferograms and maximal temporal baselines throughout the season) will be documented by coherence time series. During the documented seasons, the coherence with be averaged for all interferograms used for each considered acquisition time. As an estimate of the phase standard deviation (**Figure 2**), coherence time series at similar dates as the displacement data provides a measure of uncertainty (Balmer & Hartl, 1998) that can be used to weight the measurements in the CryoGrid model.

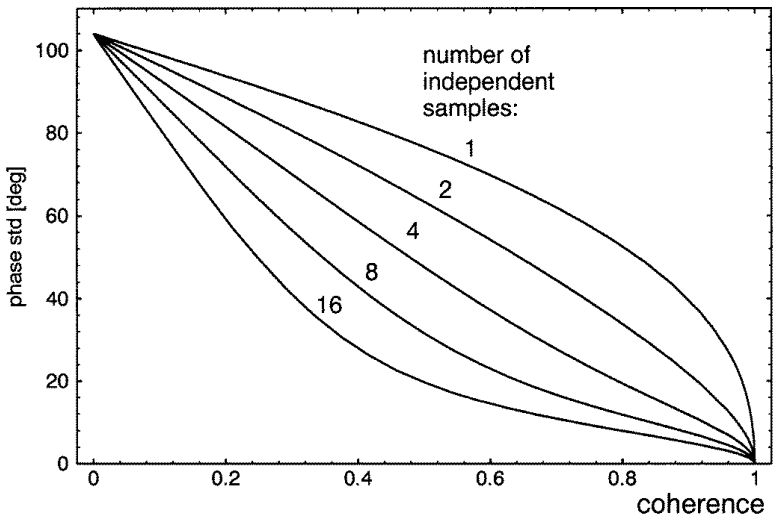

Figure 2. Interferometric phase dispersion (in degrees) as function of the interferometric coherence estimates for various multi-looking factors (Bamler & Hartl, 1998).

In addition, indirect techniques to evaluate the product quality/uncertainty may be applied. Complex spatial averaging (multi-looking) improves the signal stability and dampens the influence of unrepresentative scattering effects within resolution cells (Rouyet et al., 2021). We can evaluate these effects by testing different InSAR multi-looking factors (40–100 m of final ground resolution). In

addition, ground moisture can lead to biased InSAR results, with a potential overestimation of the subsidence (Zwieback et al., 2016). Sentinel-1 InSAR displacements can be compared with results processed with available TerraSAR-X, Radarsat-2 and ALOS-2 images to evaluate the effect of the spatial resolution and cross-validate results using different radar frequencies (Wang et al, 2020).

Finally, to evaluate the relevance of InSAR SD products as indicators of subsurface conditions (e.g., water/ice content), the results will be compared with field data documenting the geocryological properties of the active layer and upper permafrost (see Option 7 PVP).

3.2 Uncertainty of CryoGrid products

The data assimilation procedure first simulates model results for an initial ensemble of plausible input parameters which are compared to observations (i.e. InSAR SD) and assigned weights describing how likely each ensemble member is, given the observations. As main measure for uncertainty characterization, we will therefore use the standard deviation of the weighted model ensemble results after data assimilation. In practice, this will allow us to directly characterize the uncertainties for both ground temperatures and active layer thickness. However, this only works if the main sources of uncertainty for each of the variables can be included in the initial model ensemble (see above). Examples in which this may not be the case are sites with highly biased model forcing, or sites for which the selected subsurface model type does not produce realistic results.

In addition to the model-derived uncertainties, we will therefore also use the extensive database of in-situ observations of ground temperatures and active layer thickness (see Option 7 PVP). The skill of the algorithm is assessed through standard measures such as the correlation and the root mean square error.

4 ACCURACY TO BE REPORTED

The following measures of accuracy will be reported:

- **For InSAR SD products:** Coherence time series and mean coherence maps as an estimate of the phase standard deviation.
- **For point-scale simulations:** Averaged bias, mean absolute error and RMSE in °C for the ground temperature at standardized depths (daily time stamps), and in meters for the active layer thickness.
- **At the regional scale:** Ensemble spread after assimilating InSAR SD.

5 REFERENCES

5.1 Bibliography

Antonova, S., Kääb, A., Heim, B., Langer, M. & Boike, J. (2016). Spatio-temporal variability of X-band radar backscatter and coherence over the Lena River Delta, Siberia. *Remote Sensing of Environment*, 182, 169–191.

Bamler, R., & Hartl, P. (1998). Synthetic aperture radar interferometry. *Inverse problems*, *14*(4), R1.

Chen, C. W. & Zebker, H. A. (2002). Phase unwrapping for large SAR interferograms: Statistical segmentation and generalized network models. *IEEE Transactions on Geoscience and Remote Sensing*, 40(8), 1709–1719.

Crosetto, M., Monserrat, O., Bremmer, C., Hanssen, R. F., Capes, R., & Marsh, S. (2009). Ground motion monitoring using SAR interferometry: quality assessment. *European Geologist Magazine*, *26*, 12–15.

Emardson, T. R., Simons, M. & Webb, F. (2003). Neutral atmospheric delay in interferometric synthetic aperture radar applications: Statistical description and mitigation. *Journal of Geophysical Research: Solid Earth*, 108(B5).

Ferretti, A. (2014). *Satellite InSAR Data: reservoir monitoring from space (EET 9)*. EAGE Publications.

Hanssen, R. F. (2001). *Radar interferometry: data interpretation and error analysis* (Vol. 2). Springer Science & Business Media.

Kampes, B. M. (2006). *Radar interferometry* (Vol. 12). Dordrecht, The Netherlands: Springer.

Langer, M., Westermann, S., Heikenfeld, M., Dorn, W. and Boike, J., 2013. Satellite-based modeling of permafrost temperatures in a tundra lowland landscape. *Remote Sensing of Environment*, *135*, pp.12–24.

Massonnet, D., & Feigl, K. L. (1998). Radar interferometry and its application to changes in the Earth's surface. *Reviews of geophysics*, *36*(4), 441–500.

NPI (2014). Terrengmodell Svalbard (S0 Terrengmodell) [Data set]. Norwegian Polar Institute. https://doi.org/10.21334/npolar.2014.dce53a47.

Rocca, F., Prati, C., Monti Guarnieri, A., & Ferretti, A. (2000). SAR interferometry and its applications. *Surveys in Geophysics*, 21, 159–176.

Rosen, P. A., Hensley, S., Joughin, I. R., Li, F. K., Madsen, S. N., Rodriguez, E., & Goldstein, R. M. (2000). Synthetic Aperture Radar Interferometry. *Proceedings of the IEEE*, 88(3), 333–382.

Rouyet, L., Liu, L., Strand, S. M., Christiansen, H. H., Lauknes, T. R., & Larsen, Y. (2021). Seasonal InSAR Displacements Documenting the Active Layer Freeze and Thaw Progression in Central-Western Spitsbergen, Svalbard. *Remote Sensing*, *13*(15), 2977.

Zwieback, S., Liu, X., Antonova, S., Heim, B., Bartsch, A., Boike, J., & Hajnsek, I. (2016). A statistical test of phase closure to detect influences on DInSAR deformation estimates besides displacements and decorrelation noise: Two case studies in high-latitude regions. *IEEE Transactions on Geoscience and Remote Sensing*, *54*(9), 5588–5601.

Wang, L., Marzahn, P., Bernier, M., & Ludwig, R. (2020). Sentinel-1 InSAR measurements of deformation over discontinuous permafrost terrain, Northern Quebec, Canada. *Remote Sensing of Environment*, *248*, 111965.

Rouyet (2021). Ground Dynamics in the Norwegian Periglacial Environment Investigated by Synthetic Aperature Radar Interferometry. PhD dissertation. Faculty of Science and Technology, Department of Geosciences, UiT The Arctic University of Norway.

Rouyet, L., Liu, L., Strand, S. M., Christiansen, H. H., Lauknes, T. R., & Larsen, Y. (2021). Seasonal InSAR Displacements Documenting the Active Layer Freeze and Thaw Progression in Central-Western Spitsbergen, Svalbard. *Remote Sensing*, *13*(15), 2977.

Kampes, B. M. (2006). *Radar interferometry* (Vol. 12). Dordrecht, The Netherlands: Springer.

Massonnet, D., & Feigl, K. L. (1998). Radar interferometry and its application to changes in the Earth's surface. *Reviews of geophysics*, *36*(4), 441–500.

Rocca, F., Prati, C., Monti Guarnieri, A., & Ferretti, A. (2000). SAR interferometry and its applications. *Surveys in Geophysics*, 21, 159–176.

Rosen, P. A., Hensley, S., Joughin, I. R., Li, F. K., Madsen, S. N., Rodriguez, E., & Goldstein, R. M. (2000). Synthetic Aperture Radar Interferometry. *Proceedings of the IEEE*, 88(3), 333–382.

Wang, L., Marzahn, P., Bernier, M., & Ludwig, R. (2020). Sentinel-1 InSAR measurements of deformation over discontinuous permafrost terrain, Northern Quebec, Canada. *Remote Sensing of Environment*, *248*, 111965.

Westermann, S., Ingeman-Nielsen, T., Scheer, J., Aalstad, K., Aga, J., Chaudhary, N., ... & Langer, M. (2023). The CryoGrid community model (version 1.0) – a multi-physics toolbox for climate-driven simulations in the terrestrial cryosphere. *Geoscientific Model Development. 16*(9), 2607–2647.

Zebker, H. A. & Villasenor, J. (1992). Decorrelation in interferometric radar echoes. *IEEE Transactions on Geoscience and Remote Sensing*, 30(5), 950–959.

Zwieback, S. & Hajnsek, I. (2014). The impact of vegetation growth on DIn- SAR coherence regions and estimated deformations. In *Proceedings of the 2014 IEEE Geoscience and Remote Sensing Symposium*, 13–18 July 2014, Quebec, Canada (pp. 966–969).

Zwieback, S., Hensley, S. & Hajnsek, I. (2015). Assessment of soil moisture effects on L-band radar interferometry. *Remote Sensing of Environment*, 164, 77–89.

Zwieback, S., Liu, X., Antonova, S., Heim, B., Bartsch, A., Boike, J., & Hajnsek, I. (2016). A statistical test of phase closure to detect influences on DInSAR deformation estimates besides displacements and decorrelation noise: Two case studies in high-latitude regions. *IEEE Transactions on Geoscience and Remote Sensing*, *54*(9), 5588–5601.

5.2 Acronyms

AD	Applicable Document
ADP	Algorithm Development Plan
ALT	Active Layer Thickness
ATBD	Algorithm Theoretical Basis Document
B.GEOS	b.geos GmbH
CCI	Climate Change Initiative
ECV	Essential Climate Variable
EO	Earth Observation
ESA	European Space Agency
E3UB	End-To-End ECV Uncertainty Budget
GAMMA	Gamma Remote Sensing AG
GCOS	Global Climate Observing System
GT	Ground Temperature
GTN-P	Global Terrestrial Network for Permafrost
UIO	University of Oslo
INSAR	Synthetic Aperature Radar Interferometry
IPA	International Permafrost Association
NORCE	Norwegian Research Centre AS
PE	Permafrost Extent
PF	Permafrost Fraction
PSD	Product Specification Document
PVASR	Product Validation and Algorithm Selection Report
PVP	Product Validation Plan

RD	Reference Document
RMSE	Root Mean Square Error
SAR	Synthetic Aperture Radar
SD	Surface Displacement
URD	Users Requirement Document
URq	User Requirement
WMO	World Meteorological Organisation